LLNL-JRNL-412615

Experimental Verification of the Linear Theory for Stimulated Raman Scattering in High-Temperature Hohlraum Plasmas

D. H. Froula, L. Divol, R. A. London, R. L. Berger, T. Doppner, N. B. Meezan, J. S. Ross, L. J. Suter, C. Sorce, S. H. Glenzer

April 29, 2009

Physical Review Letters

Experimental Verification of the Linear Theory for Stimulated Raman Scattering in High-Temperature Hohlraum Plasmas

D. H. Froula,* L. Divol, R. A. London, R. L. Berger, T. Döppner,
N. B. Meezan, J. S. Ross,† L. J. Suter, C. Sorce, and S. H. Glenzer
L-399, Lawrence Livermore National Laboratory, P.O. Box 808, Livermore, CA 94551, USA
(Dated: April 28, 2009)

We show that the measured stimulated Raman scattering (SRS) in a large-scale high-temperature plasma scales strongly with the plasma density, increasing by an order of magnitude when the electron density is increased by 20%. This is consistent with linear theory in a uniform plasma and will set the limit on drive laser beam intensity for forthcoming ignition experiments at the National Ignition Facility. Control of SRS at laser intensities consistent with 285 eV ignition hohlraums are achieved by using polarization smoothing which increases the intensity threshold for the onset of SRS by 1.6 ± 0.2. These results were quantitatively predicted by full beam 3-dimensional numerical laser-plasma interaction simulations.

PACS numbers: 52.25.Os, 52.35.Fp, 52.50.Jm
Keywords: laser plasma instabilities, laser beam propagation, polarization smoothing, stimulated Raman scattering

In the indirect drive approach to inertial confinement fusion, a high-Z radiation cavity (hohlraum) is used to convert laser energy into soft x rays to drive a fusion capsule implosion by ablation pressure [1]. In order to produce symmetric implosions, it is critical that laser beams are able to deposit their energy near the hohlraum wall after propagating through millimeters of under-dense plasma. In current ignition designs, beams are required to propagate through a relatively uniform high-density (1.5×10^{21} cm^{-3}) moderate-temperature ($T_e = 2.5$ keV) region created by the initial low-density gas fill compressed by the expanding hohlraum wall and blow-off material from the capsule [2]. Laser intensities are kept low (mid to low 10^{14} W-cm^{-2}) to minimize laser plasma instabilities and provide an efficient heating of the hohlraum.

In a uniform plasma, linear theory suggests that the stimulated Raman scattering (SRS) reflectivity scales with the linear gain exponent which can be written for the experiments discussed in this letter as

$$G_{SRS} \simeq 0.2 \left(\frac{I}{10^{15}[\text{W-cm}^{-2}]}\right)\left(\frac{1}{\nu_e/\omega_p}\right);$$

$\nu_e/\omega_p = \sqrt{\pi/8}(k\lambda_d)^{-3}\exp\left[-\left(\sqrt{2}\,k\lambda_d\right)^{-2}\right]$ is the Landau damping where $k\lambda_d$ is the ratio of the Debye length over the wavelength of the plasma wave. Experimentally the gain can be scaled by changing the laser beam intensity or by using the strong dependence of the Landau damping on plasma density. SRS reflectivity measurements from previous studies have not followed linear theory, observing little scaling of the SRS backscatter with small variations in electron density but these studies focused primarily on higher-drive intensities well above instability thresholds and found that SRS backscatter results were dominated by filamentation [4, 5], competition with SBS [6], density gradients [7], or nonlinear saturation physics [8–10].

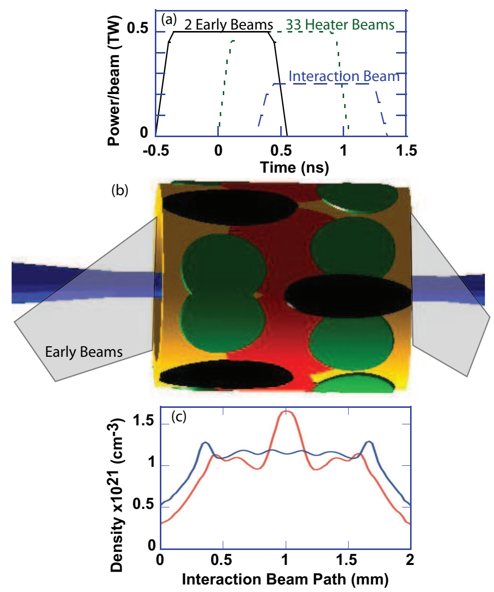

FIG. 1: (a) Beam timing; two laser beams blow-down the windows on the LEH prior to the heater beams. (b) The heater beams are uniformly distributed over the hohlraum wall using new elliptical phase plates which produces a uniform plasma density along the hohlraum axis. (c) The plasma density along the hohlraum axis is shown for conditions (blue curve) with heater beam phase plates and (red curve) without the heater beam phase plates.

In this letter, we report on the measurements of a density-dependant intensity threshold for stimulated Raman scattering in hot-uniform hohlraum plasma at intensities below the filamentation threshold, providing a strong experimental basis for ignition experiments. We have measured the SRS sensitivity to small variations in the electron plasma density and found it to be con-

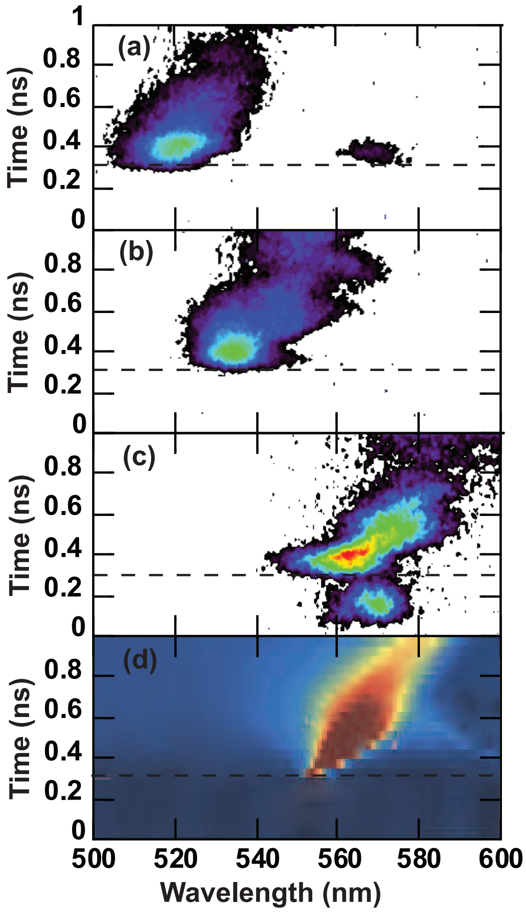

FIG. 2: The SRS spectra show that the scattered wavelength increases in time as a result of the increasing electron temperature. Furthermore, the peak wavelength increases with increasing plasma density (a) 10.1% n_{cr}, (b) 11.3% n_{cr}, (c) 13.0% n_{cr}. (d) The synthetic gain spectrum calculated by LIP is shown for a density of 11% n_{cr}.

sistent with linear theory predictions; a 20% increase in plasma density results in an order of magnitude increase in the measured SRS, as the Landau damping is divided by 3.5 while SBS remains energetically insignificant ($R_{SBS} < 1\%$).

Polarization smoothing is measured to increase the SRS intensity threshold by a factor of 1.6 ± 0.2 where the threshold for backscatter is defined as the intensity (I_{th}) at which 5% of the incident power is backscattered. These backscatter measurements are reproduced by pf3D simulations which models the laser beam propagation through the full 2-mm long plasma in three dimensions.

For this study, a novel high-density gas-filled hohlraum platform for studying laser-plasma interactions has been developed by introducing laser beams to blow-down the 260 nm thick polyimide windows covering the laser entrance holes and uniformly distributing the heater beams on the hohlraum wall [Fig. 1(b)]; this configuration created a hot uniform plasma density ($T_e \simeq 2.5$ keV, $10\% < n_e/n_{cr} < 13\%$) along the hohlraum axis by reducing the thermally-driven blast waves launched as the heater beams initially burn through the gas [Fig. 1(c)]. The density in the 1.6-mm diameter, 2-mm long hohlraum targets is varied by choosing the neopentane (C_5H_{12}) gas-fill pressure (< 1.1 ATM).

An interaction beam was aligned along the axis of hohlraum (Fig. 1) providing a direct measurement of the laser beam propagation and transmission at ignition hohlraum conditions. The hohlraum is heated by 33, 1-ns long square pulsed, frequency tripled frequency tripled ($\lambda_o = 351$ nm) laser beams (15 kJ) at the OMEGA Laser Facility [11]. The heater beams are smoothed by elliptical phase plates that project a $\sim 250\mu$m diameter intensity spot at the 1200 μm diameter laser entrance holes. The plasmas produced in these experiments are comparable to the conditions encountered by the laser beams propagating between the expanding hohlraum wall and the capsule blow-off in indirect drive ignition experiments on the National Ignition Facility [2].

Figure 2 shows that the SRS backscatter wavelength scales with the electron density inferred from the initial fill density. The peak SRS wavelength at 700 ps increases from 535 nm at an electron density of 10%n_{cr} to 580 nm at an electron density of 13%n_{cr}. The three spectra shown have an increasing intensity ($I_{10\%} = 12 \times 10^{14}$ W-cm^{-2}, $I_{11\%} = 9.5 \times 10^{14}$ W-cm^{-2}, $I_{13\%} = 4.2 \times 10^{14}$ W-cm^{-2}) as the electron density decreases and maintain a nearly constant time integrated SRS reflectivity ($R \simeq 7\%$).

The interaction beam is focused at the center of the hohlraum using an $f/6.7$ lens. A continuous phase plate (CPP) [12] was used to produce a 200 μm laser spot at best focus. The average on axis intensity at best vacuum focus for this beam is $I = 2.6 \times P$ (in GW)$\times 10^{12}$ W-cm^{-2}, where P is the incident laser beam power ranging from 50 to 500 GW. On selected shots, a birefringent polarization smoothing (PS) crystal was installed in the interaction beam path to separate the speckles in the plasma and decorrelate the speckle pattern while having minimal effect on the average intensity of the laser beam [13].

Light scattered back into the original beam cone is collected by the full-aperture backscatter station (FABS) [14]. The light backscattered outside of the FABS reflects from a plate surrounding the interaction beam and is collected by near-backscatter imager (NBI) cameras [15]. The FABS time resolves both the SBS (-0.5 nm $< \Delta\lambda_o < 1.5$ nm) and SRS (450 nm $< \lambda_{SRS} <$ 650 nm) spectrum using a 1.5 meter spectrometer and a 1/4 meter spectrometer coupled to high-dynamic-range streak cameras. The total energy is measured in both spectra using absolutely calibrated calorimeters with an uncertainty in the the total backscattered energy of 5%.

Figure 3 shows the measured density thresholds at three intensities. From this plot is is evident that in-

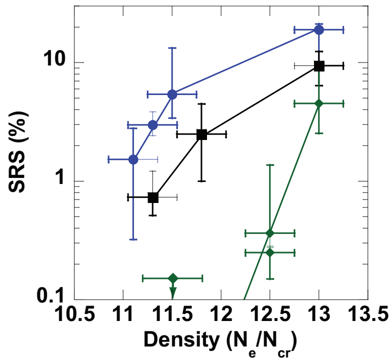

FIG. 3: The instantaneous SRS reflectivity, when full smoothing is applied (CPP & PS), is plotted as a function of the plasma density for various interaction beam intensities: (blue circles) 9×10^{14} W-cm^{-2} (black squares) 5.2×10^{14} W-cm^{-2} (green diamonds) 3.9×10^{14} W-cm^{-2}.

creasing the density by 20% reduces the intensity threshold by more than a factor of I$_{th}$(11%)/I$_{th}$(13%) $\simeq$ 2; at the highest densities tested, the intensity must remain below I$_{th}$(13%) $= 4 \times 10^{14}$ W-cm^{-2} to maintain the backscatter reflectivity below 5% while reducing the density to 11%n_{cr} allows the intensity to be increased to I$_{th}$(11%) $= 9 \times 10^{14}$ W-cm^{-2}. Our experimental findings are consistent with theoretical predictions in a uniform plasma based on Landau damping which strongly decreases with electron density in this regime. For the density range reported here, the normalized damping rate increase from $\nu_e/\omega_p = 0.01$ at n$_e$/n$_{cr}$ = 13% to $\nu_e/\omega_p = 0.035$ at n$_e$/n$_{cr}$ = 11%. Furthermore, for intensities below 9×10^{14} W-cm^{-2}, less than 10% of the backscattered energy is measured outside of the FABS which is consistent with previous experiments and being below the filamentation threshold [16].

The sensitivity of SRS to density shown in Fig. 3 indicates the importance of controlling the plasma density and the laser beam intensity in targets where SRS will adversely affect the experiment. For example, indirect drive ignition requires that the SRS remains low to prevent hot electron production [17] and to allow efficient laser beam propagation to the hohlraum wall. Current ignition designs for the National Ignition Facility [18] mitigate SRS by remaining in the strongly damped regime (k$\lambda_d > 0.4$) when the laser beam intensity is high and keeping the laser intensity below the backscatter threshold where the density is high and the temperature is low (k$\lambda_d < 0.4$).

Figure 4 shows that polarization smoothing reduces the SRS reflectivity at all times during the experiment and for all intensities. The SRS reflectivity peaks early in time as the interaction beam turns on and the plasma is still relatively cold ($T_e = 1.5$ keV). As the plasma temperature reaches its peak temperature ($T_e = 2.8$ keV), the SRS reflectivity drops below detection levels ($R < 0.01\%$).

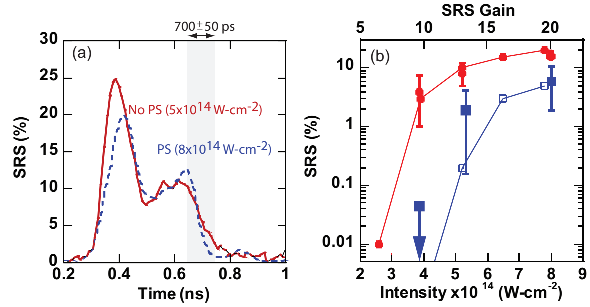

FIG. 4: (a) The measured SRS reflectivity with a CPP-smoothed beam (solid red curve) at an intensity of 5×10^{14} W-cm^{-2} is equivalent at all times to the reflectivity measured at an intensity of 7.5×10^{14} W-cm^{-2} when adding polarization smoothing (dashed blue curve).(b) The instantaneous SRS reflectivity at 700 ps is plotted as a function of the average interaction beam intensity; two laser-smoothing conditions are shown: CPP-only (red circles), CPP and PS (blue squares). Pf3d simulations calculate the measured backscatter (solid curves). All data shown is for a density of n$_e$/n$_{cr}$ = 11.5%.

Figure 4(b) shows that the intensity at which 5% of the incident power is backscattered for a CPP-smoothed laser beam is increased by a factor of 1.6 ± 0.2 when adding polarization smoothing. This novel observation shows that polarization smoothing is an effective mitigation technique for controlling stimulated Raman scattering in a high-temperature inertial confinement fusion plasma where filimentation effects are negligible.

The instantaneous backscatter is determined at a time 700 ps after the rise of the heater beams once the plasma reaches high plasma temperatures where filamentation effects are negligible [16]. Furthermore, the SRS reflectivity peaks early in time when the plasma is cold and for the lower scattering conditions (I $\lesssim 8 \times 10^{14}$ W-cm^{-2}, n$_e$/n$_{cr}$ $\lesssim$ 12%) the signal is reduced below detection level ($< 0.01\%$) when the electron temperature reaches 2.7 keV ($\sim$ 800 ps). The instantaneous reflectivity is calculated by averaging over a 100 ps range and the error bars are given by the extreme reflectivities within this range.

Simulations that calculate the interaction beam propagation and the instantaneous SRS reflectivity using the code Pf3d [19] agree well with the measured backscatter. In particular, Fig. 4(b) compares these simulations with the measured SRS backscatter and reproduces both the CPP-only results and the effects of polarization smoothing. These three-dimensional calculations use a paraxial approximation to model the whole laser beam propagating through the full 2-mm long hohlraum plasma. The code includes models for both SRS and SBS backscattering and shows that using a fluid-based modeling of SRS including linear kinetic corrections (i.e. Landau damping), coupled to accurate hydrodynamic profiles and a realistic description of the laser intensity pattern gener-

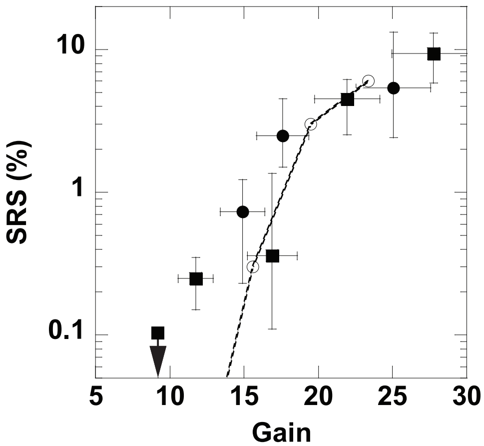

FIG. 5: The measured instantaneous SRS is plotted as a function of the linear gain exponent for intensities below 1×10^{15} W-cm^{-2} (i.e. below filimentation) and a range of densities ($\bullet$ < 12%n_{cr} < $\blacksquare$). Polarization smoothing was used on these shots. The pf3D simulations (open circles) reproduce the measured gain scaling.

ated by various smoothing techniques leads to quantitative agreement between the measurement and calculated relfectivities [20].

The bulk plasma conditions used in these simulations are calculated in two dimensions axisymmetric geometry as a function of time using the hydrodynamic code HYDRA [21]. Previous Thomson scattering studies performed at low densities ($n_e/n_{cr} = 6\%$) demonstrated that the plasma conditions were insensitive to the heat conduction models [22]; at the higher densities of this experiment the nonlocal model [23] resulted in better comparisons with the spectra data [Fig. 2(d)].

Linear theory predicts that the gain exponent for stimulated Raman scattering scales strongly with the background plasma density through the Landau damping and is linear with respect to laser intensity. Accordingly, the linear gain exponent determined by postprocessing the plasma properties from the hydrodynamic simulations using the code LIP [24] can be used to compare the measured backscatter between different experimental configurations.

Figure 5 shows that the measured SRS reflectivity scales with linear gain exponent over a wide range of densities ($10.8\% < n_e/n_{cr} < 13\%$) and intensities ($2.5 \times 10^{14}$ W-cm^{-2} < I < 9×10^{14} W-cm^{-2}). This 20% increase in the electron density corresponds to a factor of 3 decrease in the Landau damping. Furthermore, Fig. 5 demonstrates that the resulting increase in scattering can be mitigated by reducing the laser beam intensity to maintain a constant linear gain exponent. Indeed, the density thresholds ($R_{SRS} > 5\%$) measured in Fig. 3 correspond to the nearly the same linear gain ($G_{13\%} = 22$, $G_{11\%} = 24$).

LIP calculates the steady-state convective spatial growth rate for SRS as a function of the scattered light frequency using a kinetic description of the plasma susceptibilites. At each time, the total gain (G_{SRS}) is determined by integrating the growth rate along light rays taking into account the spatially varying plasma conditions The error in the calculated gains were determined by the uncertainty in heat transport models. The flux limiter was varied between $0.05 < f < 0.2$ which resulted in a 10% uncertainty in the gain.

In summary, we have demonstrated that for a hot-uniform plasma at ignition relevant plasma conditions, SRS has a strong dependence on the plasma density; increasing the plasma density by 20% results in an order of magnitude increase in SRS. Our SRS measurements agree with linear theory over a wide range of laser intensities and plasma densities. Furthermore, we have experimentally demonstrated that when using polarization smoothing the laser intensities can be increased by 60% while maintaining similar backscatter losses. These results highlight the importance of controlling the plasma density and choosing the proper laser beam intensity in future ignition target designs.

This work was performed under the auspices of the U.S. Department of Energy by Lawrence Livermore National Laboratory under Contract DE-AC52-07NA27344.

* Electronic address: `froula1@llnl.gov`
† University of California at San Diego, Mechanical and Aerospace Engineering Department

[1] J. D. Lindl *et.al.*, Phys. Plasmas **11**, 339 (2004).
[2] D. A. Callahan *et.al.*, Phys. Plasmas **13** (2006).
[3] W. L. Kruer, *The Physics of laser plasma interactions* (Addison-Wesley Publishing Company, Inc., 1988).
[4] B. MacGowan *et.al.*, Phys. Plasmas **3**, 2029 (1996).
[5] D. S. Montgomery *et.al.* Phys. Plasmas **3**, 1728 (1996).
[6] H. A. Baldis *et.al.*, Phys. Rev. Lett. **62**, 2829 (1989).
[7] W. Seka *et.al.*, Phys. Fluids **27**, 2181 (1984).
[8] J. C. Fernandez *et.al.*, Phys. Plasmas **7**, 3743 (2000).
[9] S. H. Glenzer *et.al.*, Phys. Rev. Lett. **86**, 2565 (2001).
[10] J. D. Moody *et.al.*, Phys. Rev. Lett. **86**, 2810 (2001).
[11] T. Boehly *et.al.*, et al., Opt. Comm. **133**, 495 (1997).
[12] S. Dixit *et.al.*, Opt. Lett. **21**, 1715 (1996).
[13] D. H. Froula *et.al.*, Phys. Rev. Lett. **101** (2008), aPS.
[14] S. Regan *et.al.*, Phys. Plasmas **6**, 2072 (1999).
[15] P. Neumayer *et.al.*, Rev. Sci. Instr. **79**, (2008).
[16] D. H. Froula *et.al.*, Phys. Rev. Lett. **98**, 085001 (2007).
[17] E. Dewald *et.al.*, Phys. Plasmas **13**, (2006).
[18] E. Moses *et.al.*, Fusion Sci. Technol. **47**, 314 (2005).
[19] R. L. Berger *et.al.*, Phys. Plasmas **5**, 4337 (1998).
[20] L. Divol *et.al.*, Phys. Rev. Lett. **100**, (2008).
[21] M. M. Marinak *et.al.*, Phys. Plasmas **8**, 2275 (2001).
[22] D. Froula *et.al.*, Phys. Plasmas **13**, 052704 (2006).
[23] G. P. Schurtz *et.al.*, Phys. Plasmas **7**, 4238 (2000).
[24] N. B. Meezan *et.al.*, et al., Phys. Plasmas **14**, 056304 (2007).